The Search for a Permanent Electric Dipole Moment using ^{129}Xe and ^{3}He

Rohan J. Hoare and Eduardo R. Oteiza
Harvard University, Cambridge, Massachusetts 02138 USA

Timothy E. Chupp
University of Michigan, Ann Arbor, Michigan 48109 USA

Abstract

Time reversal and parity non-invariant interactions within an atom naturally give rise to an atomic permanent electric dipole moment (PEDM). For noble gas atoms, the size of such a PEDM scales as Z^2 and higher powers of Z depending on the actual manifestation of T non-invariance, most importantly a distribution of electric dipole moment within the nucleus (Schiff Moment) and a T-odd tensor interaction between the nucleus and atomic electrons. We have developed techniques to simultaneously measure the PEDMs of ^{129}Xe and ^{3}He in a single cell in order to mitigate systematic effects due to leakage currents and common mode problems such as magnetic field and time base noise. The philosophy of our approach is that the PEDM of ^{3}He is negligible compared to that of ^{129}Xe and thus we use the ^{3}He as a "magnetometer" and monitor of systematic effects. Sensitivity of $\approx 10^{-25}$ e-cm per day has been demonstrated in preliminary work using a free induction decay tehchnique.

Introduction

The permanent electric dipole moment (PEDM) of a system is a vector quantity ($\vec{d}$) defined as the first moment of the electric charge distribution which, for a system with total angular momentum $\vec{J}$, must transform like $\vec{J}$. The permanent magnetic moment ($\vec{\mu}$) is a familiar quantity that is known to transform like $\vec{J}$, however $\vec{J}$ and $\vec{\mu}$ are axial vectors whereas $\vec{d}$ is a *polar* vector. Thus $\vec{d}$ and $\vec{J}$ do not transform in the same way under the improper transformation of Parity Inversion (P). Nor do they transform in the same way under the transformation of Time Reversal (T). The observation of a PEDM of an atom or an elementary particle (such as the neutron) would be due to interactions that are not invariant under T and P.[1] Our motivation in searching for a PEDM is that of studying the interactions that violate invariance under Time Reversal, and the searches for PEDMs have continued since the 1950's.[2]. Such interactions, described in the language of modern elementary particle physics, also violate invariance under the transformation of CP (C is the charge conjugation transformation).

The question of the symmetry of physics under the CP and T transformations is a natural one and independent of the first observation of CP non-invariance in the neutral Kaon system nearly three decades ago.[3] In atomic systems, the searches for a PEDM are currently motivated most strongly by the opportunity to discover physics beyond the Standard Model. This is because the current Standard Model picture of elementary particle interactions can accommodate CP violation in the Kaon system but predicts PEDMs much smaller than will be detectable in the near future in any system. For example, the neutron PEDM searches currently set upper limits near 10^{-25} e-cm while the Standard Model predicts values near 10^{-32} e-cm. In atoms, similar disparities exist, though Khriplovich, Sushkov and co-workers[4], have demonstrated enhancement mechanisms in atoms and nuclei. Thus experimenters hope to discover physics beyond the Standard Model by measuring PEDM's much larger than the Standard Model prediction and to clarify the theoretical picture by setting upper limits on CP non-invariant contributions which eliminate or constrain alternatives to the Standard Model. In fact several extensions of the standard model can accomodate electron and neutron PEDMs of the order of 10^{-27} e-cm, and we refer the reader to reviews by Barr and Marciano[5] and Hunter[6].

In an atom, a detectable PEDM arises becasue the atom is polarized by Time Reversal non-invariant interactions. In general, heavier atoms are more polarizable and the size of the PEDM of the atom grows as Z^2 and higher powers of Z.[7] Thus the heaviest atoms, Cs, Tl and Hg have generally been the experimenters' first choice.

Several points should be emphasized to summarize the key motivations of our work employing the comparison of ^{129}Xe and ^{3}He. First, several experimental programs have been underway and the skill, the ingenuity and the experience of every experimenter is extremely impressive. Second, there are several possible sources of a PEDM in an atom which are listed in Table 1. Third, the size of an atomic PEDM scales as Z^2 or $Z^2A^{2/3}$, depending on the source, as shown in Table 1. And fourth, certain systematic effects may be limiting other experiments' sensitivity to an atomic PEDM in the range of 10^{-27} e-cm. The comparison of ^{129}Xe with $Z = 54$ and ^{3}He with $Z = 2$ sampling the same volume (a sealed cell) at the same time is designed to greatly reduce sensitivity to the systematic effects that are common mode including bulk magnetic fields, especially those created by leakage currents present when the electric field is applied and reversed. Other common mode noise sources such as time base drift are also reduced. The Z dependence of the atomic PEDM due to any source of T non-invariance leads to an observable PEDM of ^{3}He 700 to 1000 times smaller than that of ^{129}Xe.

In Table 1. we list the several sources of a PEDM in ^{129}Xe. These include

1) the possibility of an electron PEDM (d_e),

2) T-noninvariant nuclear forces such as those inducing the neutron's PEDM (d_n) or a nuclear distribution of electric dipole moment different from the distribution of electric charge leading to a finite Schiff moment (Q_S), and

3) T-noninvariant weak neutral currents between the electrons and nucleus which may have tensor-pseudotensor character (labeled C_T) or scalar-pseudoscalar character (labeled C_S).

In terms of these sources, the atomic PEDM of ^{129}Xe in units of e-cm may be written

$$d_{Xe} = 1 \times 10^{-3} d_e + 2.7 \times 10^{-18} \frac{Q_s}{fm^3} + 5.2 \times 10^{-21} C_T + 7.5 \times 10^{-23} C_S \quad (1)$$

In Table 1 we also show the Z dependence in Xe for each source and the limits established by recent experiments.

Table 1. Sources of atomic PEDM and current limits

Source	Z dependence	Current Limit	system
Electron PEDM	$Z^3\alpha^2$ for $J \neq 0$	$d_e = -3 \pm 8 \times 10^{-27}$e-cm	Tl– beam[8]
		$d_e = -3 \pm 8 \times 10^{-26}$e-cm	Cs – cell[9]
T-nonconserving		$d_n = -3 \pm 5 \times 10^{-25}$e–cm	neutron bottle[10]
nuclear interactions	$Z^2A^{2/3}$	$Q_S = -2 \pm 4 \times 10^{-10}$e–fm^3	Hg – cell[11]
		$Q_S = \ 2 \pm 4 \times 10^{-10}$e–fm^3	TlF – beam[12]
T-nonconserving	Z^2	$C_T = -1 \pm 3 \times 10^{-7}$	Hg – cell[11]
neutral currents	Z^3	$C_S = \ 2 \pm 7 \times 10^{-7}$	Tl – beam[8]

The precession frequencies of ^{3}He and ^{129}Xe in our cells can be written

$$\omega_{Xe} = \frac{\mu_{Xe}}{\hbar I_{Xe}} |\vec{B}| + \frac{d_{Xe}}{\hbar I_{Xe}} (\vec{E} \cdot \hat{B})$$
$$\omega_{He} = \frac{\mu_{He}}{\hbar I_{He}} |\vec{B}| + \frac{d_{He}}{\hbar I_{He}} (\vec{E} \cdot \hat{B}) \quad (2)$$

where $\vec{B}$ is the sum of all bulk magnetic fields including those applied and due to leakage currents. Thus

$$\vec{B} = \vec{B}_{applied} + \vec{\epsilon}_{leak}. \quad (3)$$

The leakage current component of $\vec{B}$ is expected to change when $\vec{E}$ is reversed with respect to $\vec{B}_{applied}$ and the shift of ω_{Xe} correlated with $(\vec{E} \cdot \hat{B})$ would appear

as a false PEDM signal. The role of the ^{3}He is clear when we express the ^{129}Xe precession frequency as

$$\omega_{Xe} = \frac{\mu_{Xe}}{\mu_{He}}\omega_{He} + (\vec{E}\cdot\hat{B})[\frac{d_{Xe}}{\hbar I_{Xe}} - \frac{\mu_{Xe}}{\mu_{He}}\frac{d_{He}}{\hbar I_{Xe}}] \quad (4)$$

which is independent of any bulk magnetic field including that due to the leakage current. The principle of the ideal experiment is to measure ω_{Xe} and ω_{He} and use equation (4) to extract the PEDM signal, keeping in mind that we expect $d_{Xe} >> \frac{\mu_{Xe}}{\mu_{He}}d_{He}$. In this ideal conception of the experiment, we have not included frequency shifts due to many sources including collisions with polarized Rb, time dependent magnetic fields, and the magnetization of the ^{3}He and ^{129}Xe. These frequency shifts are discussed below.

The Free Induction Decay Experiment

Our initial approach has been to employ the Free Induction Decay (FID) technique to simultaneously measure the precession frequencies of ^{129}Xe and ^{3}He in a single cell in the presence of parallel or anti-parallel applied magnetic and electric fields. The apparatus is shown in Figure 1. The ^{129}Xe and ^{3}He are contained in a cell which also contains a small amount of Rb and several hundred torr of N_2. The Rb is optically pumped with light from a Ti-sapphire laser and polarization is transferred from the Rb to the noble gas nuclei by spin exchange.[13,14] This spin exchange is mediated by a contact hyperfine interaction which is enhanced during a collision due to effects which are much stronger for the ^{129}Xe-Rb collisions than for the ^{3}He-Rb collisions.[15] The enhancement also leads to frequency shifts for ^{129}Xe and ^{3}He in the presence of polarized Rb which do not scale with the magnetic moment. Such shifts lead to modification of equation (4) as discussed below.

The cells consist of a glass cylinder about 0.8 cm long (made of Schott 8290) with glass end plates (Schott Tempax) and Molybdenum wire mesh electrodes sandwiched between the end plates and cylinder. The cylinder walls are coated with octadecyltrichlorosilane and the end caps and mesh are attached with epoxy. The challenge of producing these cells was immense and took more than one year because they must satisfy the following requirements: (1) the cells must hold off about 2 kV; (2) the ^{3}He and ^{129}Xe relaxation times must be 10 hours and 0.3 hours respectively for T_1 and at least 0.3 hours for T_2; (3) the cells must remain mechanically intact and maintain the relaxation times during thermal cycling between 120 C and 80 C; (4) all materials must be inert to Rb in the operating temperature range. Detailed information on cell construction will be available when Eddie Oteiza finishes his dissertation.[16]

The laser polarizes the Rb and the noble gas nuclei parallel (or anti-parallel) to $\vec{B}_{applied}$. We begin a run cycle by pumping for several hours at a temperature of 120C in order to build up the ^{3}He polarization to about 10%. Then the cell

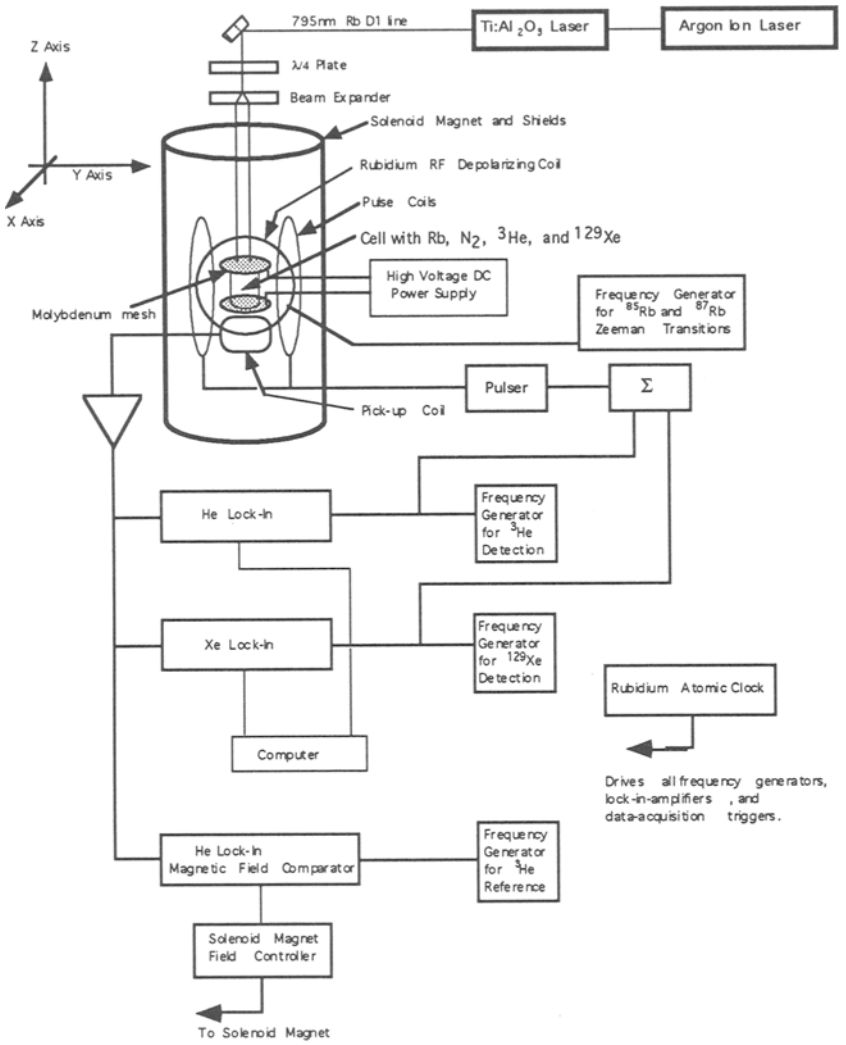

Figure 1. Schematic diagram of the apparatus for the Free Induction Decay set-up.

is cooled to 80C, a temperature at which the ^{3}He polarization relaxation time is about 10 hours and the ^{129}Xe relaxation time is about 0.3 hours (1000 seconds). A measurement is initiated by applying resonant oscillating magnetic field pulses simultaneously to both species (about 3 kHz and 10 kHz respectively for ^{129}Xe and ^{3}He) which tip the spins by 90° for ^{129}Xe and 10-30° for ^{3}He. The spins then precess freely and the precessing magnetization is detected inductively by a pick-up coil near the grounded electrode. The pick-up coil signal is amplified and distributed to mixers from which beat frequencies between the two species and reference oscillators are derived and acquired by computer. The ^{3}He signal is used in two feed back loops one which controls the magnetic field by locking up the ^{3}He Larmor frequency, and a second which provides a frequency proportional to the ^{3}He frequency, but divided down so that it is near the ^{129}Xe precession frequency.[17] The experiment's time base is provided by a commercial Rb atomic clock.

Beat frequency signals for the two species are shown in Figure 2 along with Fast Fourier Transforms (FFT) of those signals. The FFTs are shifted by the reference frequencies for the two and show that the ^{129}Xe line width is a bit broader than that for the ^{3}He, a consequence of the shorter coherence time, T_2. Also note that the magnet control loop locked the ^{3}He frequency to 9726 Hz exactly. The precision we expect for a frequency measurement is given in terms of the coherence line width and the ratio of signal to noise for the measurement by

$$\sigma_\omega = \frac{\Gamma}{S/N} \tag{5}$$

which basically defines S/N for the measurement. However, N should be dominated by random *i.e.* white noise sources, and it is proportional to $(BW)^{1/2}$ and therefore $\Gamma^{-1/2}$. There is therefore great advantage to long coherence times and correspondingly small line widths. Typical precision for a 1000 second measurement is $\sigma_\omega/2\pi \approx 100nHz$ corresponding to $S/N \approx 500/\sqrt{Hz}$. Our record for precision is $\sigma_\omega/2\pi = 50nHz$.

The free precession frequencies of ^{3}He and ^{129}Xe are extracted from the time domain signals by a least squares fitting to the model

$$S(t) = A_0 + A_1 cos(\omega t + \phi)e^{-\Gamma_2 t} \tag{6}$$

where A_0 accounts for any offset in the electronics, ω is the beat frequency and $\Gamma_2 = 1/T_2$ is the coherence decay rate. The effectiveness of our techniques of magnetic field locking and extraction of the free precession frequency is illustrated in Figure 3. Here we show the ^{3}He precession frequency extracted over one cycle of 12 runs. As expected, the ^{3}He frequency is constant indicating that the lock loop is operating well. Also apparent is the size of the frequency error

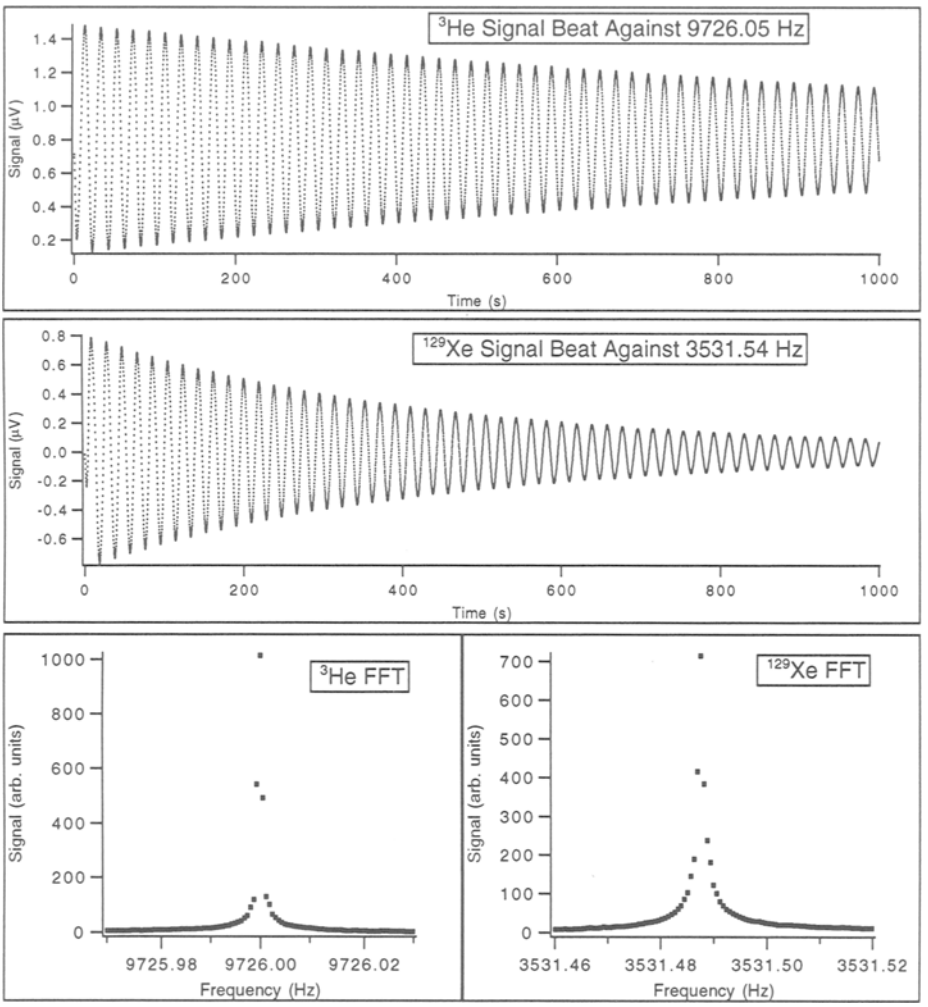

Figure 2. Beat signals for ^{3}He and ^{129}Xe in the time and frequency domains. The magnetic field is controlled to maintain the ^{3}He precession frequency at 9726 Hz.

bar which is consistent with the scatter of the extracted frequencies for each run. Thus by examining the ^{3}He frequency data, we have confidence that our PEDM measurement in the ^{129}Xe channel is accurate and that the assigned uncertainty is valid. In figure 3 we also show data for ^{129}Xe precession frequency during the same run cycle. In this case, the drift of the ^{129}Xe frequency is due to the frequency shifts discussed in the next section.

We have investigated the rejection of magnetic field contributions due, for example to leakage currents. A modulation of the current to the solenoid was effect with the ^{3}He feedback loop open (no magnet control) and closed (magnetic field locked to maintain constant ^{3}He frequency). With the loop open, the frequency modulation is 10 mHz and with the loop closed, a limit of 10 μHz demonstrated a factor of greater than 1000 rejection of magnetic field variations. If we use the typical leakage current of 10 pA and assume this current completes full loop around our cell, the resulting magnetic field would produce a false PEDM frequency shift of 10 nHz corresponding to a PEDM of 10^{-27} e–cm. With the 1000-fold rejection provided by ^{3}He magnetometry, this false PEDM signal is reduced to 10^{-30} e–cm! This clearly demonstrates the importance of our approach.

Frequency Shifts

Frequency shifts of the ^{129}Xe and ^{3}He limit the sensitivity to a PEDM. Two sorts of shifts must be considered: shifts that that correlate with the electric field reversal and thus appear as a false PEDM signal and shifts that are not correlated, but are not stable and therefore produce frequency noise and limit the precision of our measurement. The magnetic field is locked to maintain the ^{3}He free precession frequency constant and therefore any frequency shifts of the either the ^{3}He or ^{129}Xe appear in the ^{129}Xe frequency given by equation (4) by adding the term

$$(\vec{A} \cdot \hat{B})(k_{Xe} - \frac{\mu_{Xe}}{\mu_{He}} k_{He}) \tag{7}$$

where $\vec{A}$ represents any field which couples to the noble gas spin with strength k. (Both the PEDM coupling and leakage current effects have the form of equation (8), however in the case of the magnetic field due to a leakage current, $k_{Xe}/k_{He} = \mu_{Xe}/\mu_{He}$, and the shift vanishes.)

We have studied frequency shifts due to the following interactions:

None of these sources of frequency shift lead to a false PEDM signal, however they do introduce frequency noise. The largest sources of frequency noise are items 1) and 2). These shifts are large, time dependent and change abruptly every time a run is initiated, since the noble gas magnetization is rotated at the start of each run. It is therefore crucial that the electric field be reversed more frequently than once per run, which has the disadvantage that the effective

1) The hyperfine contact interaction between the noble gas nucleus and the Rb electron spin which is polarized by spin exchange from the polarized ^{129}Xe and ^{3}He leads to a shift that is about 100 times greater for ^{129}Xe. We quench the Rb polarization with resonant RF so that this shift is less than 10 μHz.

2) The longitudinal magnetization of the ^{129}Xe and ^{3}He produces a frequency shift due to the torque the resulting magnetic field exerts on the noble gas magnetic moments. For a spherical cell, the average torque on the ^{129}Xe magnetic moment due to the ^{129}Xe magnetization vanishes since the average magnetic moment is parallel to the magnetization. This is not the case for the torque on the ^{129}Xe magnetic moment due to the ^{3}He magnetization and conversely, and small

corrections for the cylindrical cell are also necessary. These shifts are estimated to be as large as 250 μHz for the ^{129}Xe and 30μ Hz for the ^{3}He.

3) Any rotating magnetic field with frequency ω_T causes a shift proportional to $(\mu_{\mathrm{Xe}} B_T)/(\omega_{\mathrm{Xe}} - \omega_T)$ for ^{129}Xe and similarly for ^{3}He. This is a generalization of the Bloch-Siegert shift for which $\omega_T = -\omega_{\mathrm{Xe}}$. Since the ^{129}Xe and ^{3}He frequencies are different, these shifts due to any rotating or oscillating magnetic field are in general different. These fields include the oscillating Rb quenching fields, and the rotating fields due to the precessing ^{129}Xe and ^{3}He magnetization. The estimated shifts are about 0.2μHz and $<<$ 1 nHz respectively for the two sources.

4) Gradients of static and rotating magnetic fields also induce shifts, which we estimate to be less than about 10 nHz.

5) The wall interactions of ^{129}Xe and ^{3}He are temperature dependent, and we have determined that the shifts are less than 0.1 μHz for a temperature change of 0.1 K.

coherence time becomes less, and therefore σ_ω increases. When the electric field is reversed in conjunction with the initiation of each run by resonant NMR pulses, we find that this frequency noise limits the sensitivity to $\sigma_\omega/2\pi = 2 \times 10^{-7} Hz/\sqrt{\mathrm{day}}$. This is a full factor of 10 worse than that expected based on the precision attained for a single run. For $|\vec{E}| = 2$ kV/cm, this limits us to a PEDM sensitivity of $\sigma_d = 2 \times 10^{-25}$ e-cm/$\sqrt{\mathrm{day}}$.

New Techniques

Improved sensitivity requires one or more of the following improvements: 1) increased T_2 for both ^{129}Xe and ^{3}He, 2) enhanced signal to noise ratio, and 3) mitigation of noise due to frequency shifts. Our experience suggests that

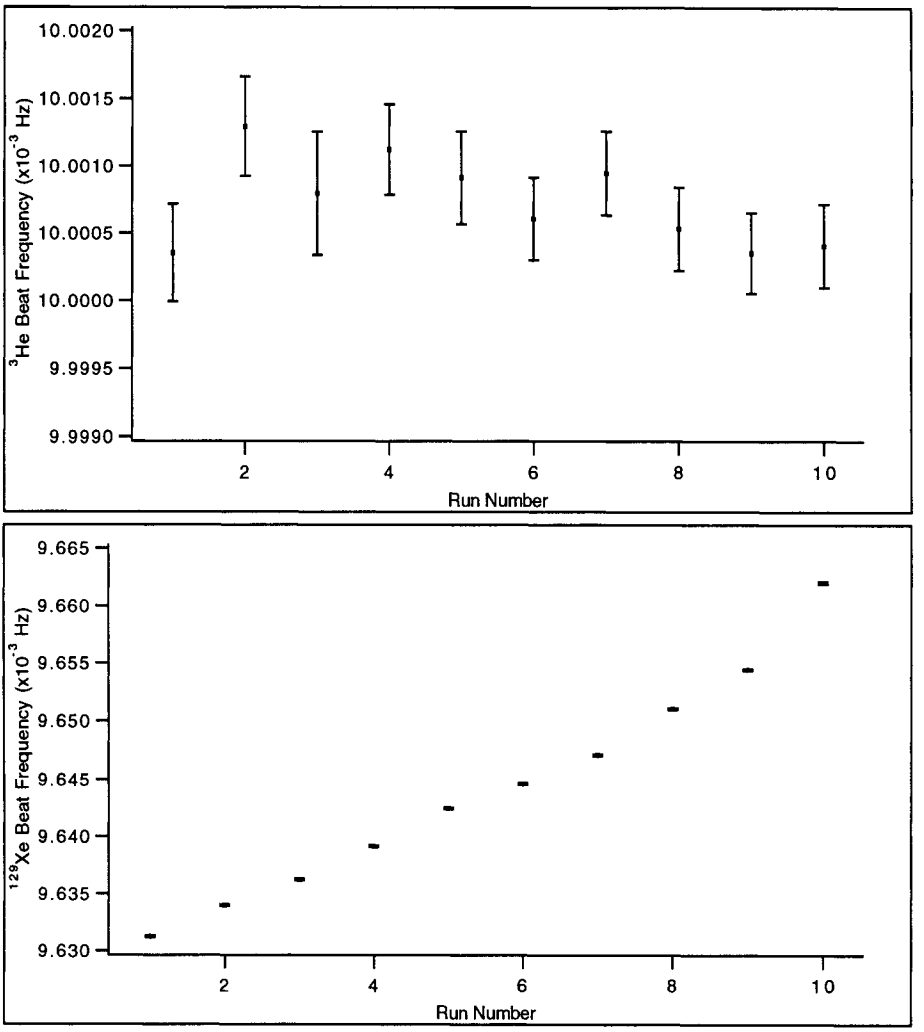

Figure 3. Beat frequencies extracted for the ^{3}He (top panel) and ^{129}Xe (bottom panel) for a single cycle of 10 runs. The ^{3}He frequency is held fixed by the magetic field control loop. The shifts in the ^{129}Xe beat frequency are due mainly to the Rb polarization and longitudinal component of the ^{3}He magnetization as discussed in the text.

increased T_2 for ^{129}Xe is probably not easy. Increased signal to noise and mitigation of frequency noise are likely to be fruitful. We are pursuing two new variations that maintain the principle of comparison of ^{129}Xe and ^{3}He. One, the exploitation of a noble gas maser[18,19] uses many of the features of the FID technique, but employs a CW maser established by the coupling of the noble gas spins to resonant pick-up coils. The second employs an optically pumped Rb magnetometer to detect the precession noble gas spins.

The maser technique promises greater signal to noise and the stability of the CW maser, in marked contrast to the Free Induction Decay. We have successfully established CW masing of ^{3}He polarized by spin exchange and used double cell techniques[20] analogous to the two bulb maser set-up. In the maser experiment, the cell in which the PEDM measurement is effected is at room temperature and therefore significantly higher electric fields can be applied than in the FID technique. We also eliminate the need for thermal cycling necessary for optimum ^{3}He and ^{129}Xe polarization in the single cell set-up.

Used as a magnetometer the Rb is sensitive to the precessing nuclear spins by way of the contact hyperfine interaction discussed above. This technique has the potential of significantly greater S/N and has been used to detect the simultaneous precession of ^{129}Xe and ^{3}He at 0.03 and 0.1 Hz respectively. Our estimates suggest that $S/N \approx 10,000\sqrt{Hz}$ or greater are attainable, but that several noise sources including laser and magnetic field stability must be eliminated.

Conclusion

Our current highest priority is to push the FID technique to its limit which we estimate to be of order 10^{-27} e-cm. In order to achieve this potential, the ^{129}Xe frequency must be consistently determined with precision 0.1 μHz for each 1000 second run. This is possible only if noise due to frequency shifts is effectively reduced below this level. Even random frequency shifts (i.e. uncorrelated with the electric field reversal) contribute to the noise spectrum from which we seek to extract the PEDM signal. It is therefore crucial to understand these shifts and render the experiment insensitive to them. For the FID technique, modulating the electric field through several cycles in the course of a single coherence time is promising though the sensitivity for a given measurement interval is reduced by the number of modulation cycles per free induction decay. Maser and optical detection techniques both promise significant improvement that should increase the sensitivity of our experiments beyond 10^{-27} e–cm with the crucial advantage of using the two species ^{3}He and ^{129}Xe.

References

1. R.G. Sachs, **The Physics of Time Reversal**, Univ. of Chicago Press, Chicago, (1987).
2. E.M. Purcell and N.F. Ramsey, Phys. Rev. **78**, 807 (1950).

3. J.H. Christenson, J.W. Cronin, V.L. Fitch, R. Turlay, Phys. Rev. Lett. **13** 138 (1964).
4. V.V. Flambaum, I.B. Khriplovich, O.P. Sushkov, Phys. Lett. **162B**, 213 (1985).
5. S.M. Barr and W.J. Marciano, in **CP Violation**, edited by C. Jarlskog, World Scientific, Singapore (1989).
6. L.R. Hunter, in **Atomic Physics 12**, edited by J. Zorn and R. Lewis, AIP, New York, 429 (1991).
7. P.G.H. Sandars, in **Atomic Physics 9**, edited by R.S¿ van Dyck and E.N. Fortson, World Scientific, New Jersey, (1985).
8. K. Abdullah, C. Carlberg, E.D. Commins, H. Gould, S. Ross, , Phys. Rev. Lett. **65** 2347 (1990).
9. S. Murthy, D. Krause,Jr., A. L. Li, L.R. Hunter , Phys. Rev. Lett. **63**, 965 (1989).
10. K. Smith, *et al.*, Phys. Lett. **B234**, 191 (1990). I.S. Altarev *et al* JETP Lett **44** 460 (1986).
11. S.K. Lamoreaux, J.P. Jacobs, B.R. Heckel, F.J. Raab, E.N. Fortson, Phys. Rev. Lett. **59**, 2275 (1987).
12. D. Cho, K. Sangster, E.A. Hinds, Phys. Rev. Lett. **63**, 2559 (1989).
13. X. Zeng, A. Wu, T. Call, E. Miron, D. Schreiber, W. Happer, Phys. Rev. **A31**, 260 (1985).
14. T.E. Chupp, M.E. Wagshul, K.P. Coulter, A.B. McDonald, W. Happer, Phys. Rev. **C36**, 2244 (1987).
15. R.M. Herman, Phys. Rev. **A137**, 1062 (1965).
16. E.R. Oteiza, private communication.
17. T.E. Chupp, E.R. Oteiza, J.M. Richardson, T.R. White, Phys. Rev. **A38**, 3998 (1988). T.E. Chupp, R.J. Hoare, R.A. Loveman, E.R. Oteiza, J.M. Richardson, M.E. Wagshul, A.K. Thompson, Phys. Rev. Lett. **63**, 1541 (1989).
18. H.G. Robinson, M.T. Myint, Appl. Phys. Lett. **5**, 116 (1964). M.T. Myint, PhD dissertation, Harvard University, 1966 (unpublished).
19. M.E. Wagshul, R. Walsworth, T.E. Chupp, private communication.
20. T.E. Chupp, R.A. Loveman, A.K. Thompson, A.M. Bernstein, D.R. Teiger, Phys. Rev. **C45**, 915, (1992).